

Optical and Magnetic Properties of some $REZnPnO$ ($Pn = P, As, Sb$) Phases

Inga Schellenberg^a, Hannes Lincke^a, Wilfried Hermes^a, Volker Dittrich^b, Robert Glaum^b, Manfred H. Möller^a, and Rainer Pöttgen^a

^a Institut für Anorganische und Analytische Chemie, Westfälische Wilhelms-Universität Münster, Corrensstraße 30, 48149 Münster, Germany

^b Institut für Anorganische Chemie, Rheinische Friedrich-Wilhelms-Universität, Gerhard-Domagk-Straße 1, 53121 Bonn, Germany

Reprint requests to R. Pöttgen. E-mail: pottgen@uni-muenster.de

Z. Naturforsch. **2010**, *65b*, 1191–1198; received May 3, 2010

Several $REZnPnO$ phases of the $ZrCuSiAs$ type (RE = rare earth element, $Pn = P, As, Sb$) were synthesized in X-ray-pure form in $NaCl/KCl$ salt fluxes. The structure of $PrZnSbO$ was refined from single-crystal diffractometer data: $P4/nmm$, $a = 418.79(8)$, $c = 946.7(5)$ pm, $wR2 = 0.0349$, 192 F^2 values, 12 parameters. The $REZnPnO$ pnictide oxides were studied with respect to magnetic susceptibility, ^{121}Sb Mössbauer spectroscopy, and optical properties.

Key words: Arsenide Oxide, Antimonide Oxide, Rare Earth, Optical Properties, Mössbauer Spectroscopy, Magnetism

Introduction

The chemistry of the quaternary pnictide oxides $RETPnO$ (RE = rare earth element; T = late transition metal; $Pn = P, As, Sb$), which were first reported 15 years ago, has gained a true renaissance in the last three years due to the outstanding physical properties of these systems [for recent reviews see 1–7]. Several of the iron-based compounds show charge density waves (antiferromagnetic ordering of the iron atoms) at temperatures around 140 K. Upon O^{2-}/F^- substitution the magnetic ordering collapses and superconductivity is observed with transition temperatures as high as 55 K ($SmFeAsO_{1-x}F_x$) [8].

Chemical bonding in the $RETPnO$ compounds can to a first approximation be understood by a simple ionic formula splitting $RE^{3+}T^{2+}Pn^{3-}O^{2-}$, leading to an electron-precise description. Similar to the large series of mixed chalcogenides $RETSO$ and $RETSO$ [9], also some of the $RETPnO$ phases are semiconductors. Our recent salt flux synthesis of the $REZnPO$ [10, 11] and $REZnAsO$ [12] series revealed yellow to dark-red, transparent single-crystals of which the optical properties were studied by single-crystal absorption spectra, confirming the optical band gaps.

In continuation of our systematic studies of structure-property relationships of quaternary pnictide ox-

ides [13], we herein report on the diverse properties of quaternary compounds from the series $REZnPnO$ ($Pn = P, As, Sb$). Some structural data on $REZnAsO$ [14] and $REZnSbO$ [15] have already been reported by the Jeitschko group, and some preliminary magnetic data were published by Takano *et al.* [16].

Experimental Section

Synthesis

Starting materials for the preparation of the pnictide oxides $REZnPnO$ ($RE = La-Nd, Sm, Gd, Tb, Er, Tm$; $Pn = P, As, Sb$) were ingots of the rare earth elements (Honeywell, Smart Elements, Chempur, or Kelpin, > 99.9%), gadolinium powder (Sigma Aldrich, 99.9%), ZnO (Chempur > 99.5%), red phosphorus (Hoechst, Knapsack, ultrapure), arsenic pieces (Sigma-Aldrich, 99.999%), antimony shots (Riedel-de Häen, 99.9%), $NaCl$ (Merck, > 99.5%) and KCl (Chempur, 99.9%). The arsenic was purified by fractional sublimation under vacuum. First, As_2O_3 was sublimed with the hot end of the sealed silica tube at 570 K and the other end at r. t. After separation of the cold end containing the sesquioxide, the tube was sealed again, and the arsenic was sublimed with the hot end of the tube at 870 K. Small pieces of the rare earth metals were first arc-melted [17] to buttons under an argon atmosphere of *ca.* 600 mbar. The argon was purified with titanium sponge (870 K), silica gel and molecular sieves.

Table 1. Crystal data and structure refinement for PrZnSbO.

Compound	PrZnSbO
Structure type	ZrCuSiAs
Space group; Z	$P4/nmm$; 2
Molar mass, g mol ⁻¹	344.03
Unit cell dimensions, pm	$a = 418.79(8)$
(Guinier data)	$c = 946.7(5)$
Calculated density, g cm ⁻³	6.88
Crystal size, μm^3	$20 \times 40 \times 45$
Detector distance, mm	60
Exposure time, min	6
ω range; increment, deg	$0 - 180^\circ$; 1.0°
Integr. param. A, B, EMS	12.5; 2.5; 0.014
Transm. ratio (max/min)	2.24
Absorption coefficient, mm ⁻¹	29.4
$F(000)$, e	296
θ range, deg	4° to 31°
Range in hkl	$\pm 6, \pm 6, \pm 13$
Total no. reflections	1922
Independent reflections / R_{int}	192 / 0.0568
Reflections with $I \geq 2\sigma(I) / R_\sigma$	141 / 0.0527
Data / ref. parameters	192 / 12
$R1 / wR2$ for $[I \geq 2\sigma(I)]$	0.0207 / 0.0294
$R1 / wR2$ for all data	0.0447 / 0.0349
Goodness-of-fit on F^2	0.678
Extinction coefficient	0.0019(7)
Largest diff. peak / hole, e \AA^{-3}	1.75 / -2.66

The small rare earth metal buttons, zinc oxide and powder of antimony, arsenic and phosphorus, respectively, were weighed in the ideal 1 : 1 : 1 atomic ratio, and 0.5 g of each mixture was sealed in an evacuated quartz ampoule together with ca. 2 g of an equimolar NaCl/KCl mixture acting as a flux medium. The mixtures were first heated at 770 K for one day, followed by longer annealing at 1120–1170 K (6–24 d). Then the reaction mixture was cooled to r. t. at a rate of 5 K/h.

Lamellar crystals were isolated from the reaction mixtures by extraction of the salt flux with hot demineralized water. Well shaped crystals (with edge lengths up to 1 mm) were obtained. Crystals of the phosphide oxides and arsenide oxides were generally suitable for measurements of their polarized single-crystal UV/Vis/NIR spectra. In case of the antimonide oxides the spectra showed strong interference effects. Thus observation of the characteristic f - f electronic transitions was hampered. All samples are stable in air for months.

Alternatively the REZnAsO ($RE = \text{Ce-Nd, Sm, Gd}$) and REZnSbO ($RE = \text{La-Nd}$) samples could be synthesized by a ceramic method. The rare earth elements were used in the form of filings, which were prepared under dry paraffin oil and subsequently washed with dry hexane. Gadolinium powder was purchased. Filings of the rare earth element and powders of zinc oxide and arsenic, respectively antimony, in the ideal 1 : 1 : 1 ratio were ground together thoroughly and cold-pressed to a pellet, which was placed in a tantalum cru-

Table 2. Atomic coordinates and displacement parameters (pm²) for PrZnSbO. U_{eq} is defined as one third of the trace of the orthogonalized U_{ij} tensor. $U_{12} = U_{13} = U_{23} = 0$.

Atom	W. site	x	y	z	$U_{11} = U_{22}$	U_{33}	U_{eq}
Pr	2c	1/4	1/4	0.11839(9)	51(3)	48(4)	50(2)
Zn	2b	3/4	1/4	1/2	113(5)	160(9)	128(4)
Sb	2c	1/4	1/4	0.68383(13)	92(4)	75(5)	87(3)
O	2a	3/4	1/4	0	130(30)	15(44)	92(19)

Table 3. Interatomic distances (pm) for PrZnSbO. All distances within the first coordination spheres are listed. Standard deviations are all equal or smaller than 0.1 pm.

Pr:	4	O	237.5	Sb:	4	Zn	272.3
	4	Sb	350.4		4	Pr	350.4
Zn:	4	Sb	272.3	O:	4	Pr	237.5

cible and sealed in an evacuated quartz ampoule. The samples were annealed at 770 K for 1 d and at 1170 K for 4 d. After this step the samples were ground again, re-pressed to pellets and re-heated at 1170 K for 4 d. Thus polycrystalline phase-pure samples were obtained which were suitable for magnetic measurements.

X-Ray diffraction

The polycrystalline samples were characterized by X-ray powder diffraction (Guinier technique, imaging plate detector, Fujifilm BAS-1800 readout system) using $\text{CuK}\alpha_1$ radiation and α -quartz ($a = 491.30$ and $c = 540.46$ pm) as an internal standard. The lattice parameters were refined from the powder data by a least-squares routine. The correct indexing was ensured through intensity calculations [18]. In all cases our refined parameters agreed with the literature data [2, 14–16] within the standard deviations.

A platelet-like crystal of PrZnSbO was selected from the sample prepared by a salt flux. The quality of the crystal was checked by Laue photographs on a Buerger camera (white Mo radiation). Intensity data were measured at r. t. using a Stoe IPDS-II imaging plate diffractometer in oscillation mode (graphite-monochromatized $\text{MoK}\alpha$ radiation). A numerical absorption correction was applied to the data set. All relevant details concerning the data collection and evaluation are listed in Table 1.

Structure refinement

In agreement with our previous studies, the systematic extinctions of the PrZnSbO data set were compatible with space group $P4/nmm$. The atomic parameters of LaZnSbO [13] were then taken as starting values, and the structure was refined using SHELXL-97 [19] (full-matrix least-squares on F^2) with anisotropic atomic displacement parameters for all atoms. Refinement of the occupancy parameters indicated no deviations from the ideal composition. The final difference

Fourier synthesis was flat (Table 1). The positional parameters and interatomic distances are listed in Tables 2 and 3.

Further details of the crystal structure investigation may be obtained from Fachinformationszentrum Karlsruhe, 76344 Eggenstein-Leopoldshafen, Germany (fax: +49-7247-808-666; e-mail: crysdata@fiz-karlsruhe.de, http://www.fiz-informationsdienste.de/en/DB/icsd/depot_anforderung.html) on quoting the deposition number CSD-380342.

Optical measurements

Crystals of the pnictide oxides *REZnPnO* show red, deep violet-red and red-brown colors depending on the crystal size and crystal structure. Whereas the *REZnPO* compounds are perfectly transparent, the corresponding *REZnAsO* compounds are less transparent and have a darker color. For the antimonide oxides *REZnSbO* hardly any transparency can be observed. These colors have repeatedly been observed for different samples.

Single-crystal electronic absorption spectra were measured at 293 K in the NIR/Vis region ($6000\text{--}25000\text{ cm}^{-1}$, step width $\Delta\lambda(\text{Vis}) = 1\text{ nm}$, $\Delta\lambda(\text{NIR}) = 2\text{ nm}$) using a strongly modified CARY 17 microcrystal spectrophotometer (Spectra Services, ANU Canberra, Australia [20, 21]). Typically, plate-like crystals (*//* to the tetragonal *ab* plane) with edge lengths around $0.2 \times 0.2 \times 0.05\text{ mm}^3$ were selected for the investigations. The spectra show the absorbance $A = -\lg(I_{\text{crystal}}/I_{\text{reference}})$ versus the wavenumber $\tilde{\nu}$. The reference intensity was measured using a pinhole instead of a crystal mounted on an aperture.

^{121}Sb Mössbauer spectroscopic measurements

A $\text{Ba}^{121m}\text{SnO}_3$ source was used for the Mössbauer spectroscopic experiments, and the quoted values of the isomer shifts are given relative to this material. The measurements were carried out in the usual transmission geometry at 77 and 4.2 K. A helium bath cryostat was used to reach 4.2 K. The temperature was controlled by a resistance thermometer ($\pm 0.5\text{ K}$ accuracy), and the Mössbauer source was kept at r. t. The samples were enclosed in small PVC containers at a thickness corresponding to about 10 mg Sb/cm^2 . The total counting time was approximately 1 d per spectrum. Fitting of the spectra was performed with the NORMOS-90 program system [22].

Magnetic susceptibility measurements

The *REZnAsO* ($RE = \text{Ce, Pr, Nd, Sm, Gd}$) samples were packed in kapton foil and attached to the sample holder rod of a VSM for measuring the magnetic properties in a Quantum Design Physical-Property-Measurement-System in the temperature range 3.1–305 K with magnetic flux densities up to 80 kOe.

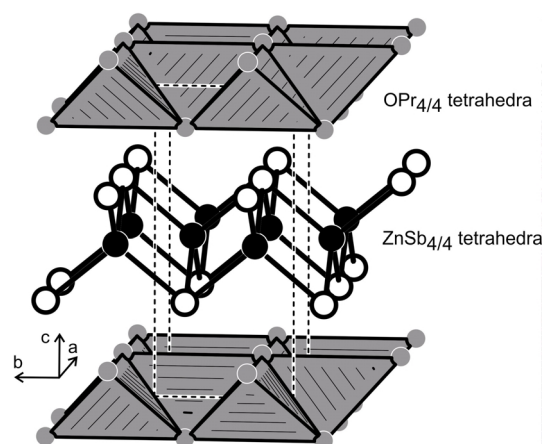


Fig. 1. The crystal structure of PrZnSbO. Praseodymium, zinc, and antimony atoms are drawn as medium grey, black filled, and open circles, respectively. The $(\text{Pr}^{3+}\text{O}^{2-})$ and $(\text{Zn}^{2+}\text{Sb}^{3-})$ layers and the tetrahedral oxygen and zinc coordination are emphasized.

Discussion

Crystal chemistry

The *REZnAsO* arsenide oxides and *REZnSbO* antimonide oxides crystallize with the tetragonal ZrCuSiAs-type structure, space group $P4/nmm$. The structure of PrZnSbO is presented in Fig. 1 as an example. It is built up from two different layers, $(\text{Pr}^{3+}\text{O}^{2-})$ and $(\text{Zn}^{2+}\text{Sb}^{3-})$, in ABAB stacking sequence. The oxygen and zinc atoms have tetrahedral coordination by praseodymium and antimony, respectively. In the *REZnPO* series [10, 15] one observes a switch in structure type. $\alpha\text{-LaZnPO}$, $\alpha\text{-CeZnPO}$ and $\alpha\text{-PrZnPO}$ adopt the ZrCuSiAs type, while $\beta\text{-CeZnPO}$, $\beta\text{-PrZnPO}$, and the *REZnPO* phases with the smaller rare earth atoms crystallize with the rhombohedral NdZnPO structure. The crystal chemical relationship between these different modifications and the chemical bonding peculiarities have been reported earlier. For details we refer to our previous work [10, 11, 15]. Herein we mainly focus on the properties of these materials.

Magnetic properties

The temperature dependence of the reciprocal magnetic susceptibility of the *REZnAsO* samples ($RE = \text{Ce, Pr, Nd, Sm, Gd}$) measured with an external applied field of 10 kOe are presented in Figs. 2 and 3. Above 100 K we observe Curie-Weiss behavior with experimental effective magnetic moments (Table 4) close

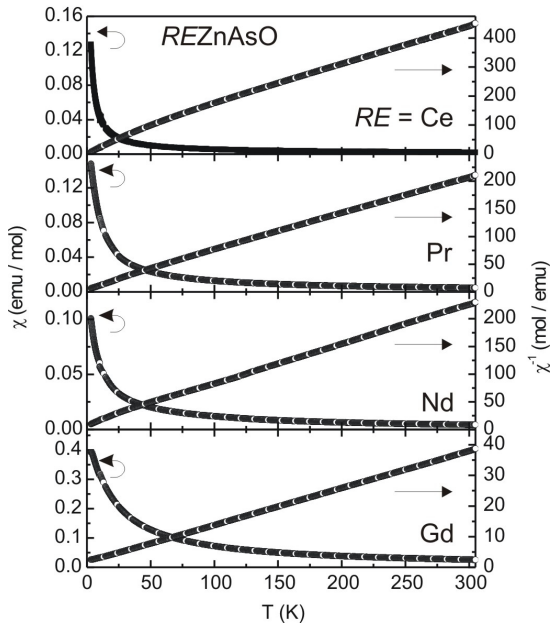


Fig. 2. The dc susceptibility (χ and χ^{-1} data) of *REZnAsO* ($RE = \text{Ce-Nd, Gd}$) measured in ZFC state of the sample at 10 kOe.

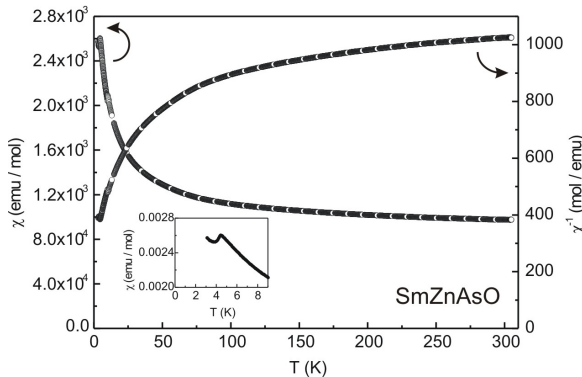


Fig. 3. Temperature dependence of the magnetic susceptibility (χ and χ^{-1} data) of *SmZnAsO* measured at a magnetic flux density of 1 T. The inset highlights the low-temperature susceptibility features of *SmZnAsO* below 9 K.

to the free ion values, respectively, similar to the reported ones [16] for *REZnAsO* ($RE = \text{Ce, Pr, Nd}$). The magnetic susceptibility of *SmZnAsO* does not follow a Curie-Weiss law, as could be expected for a compound containing the Van Vleck ion Sm^{3+} . Antiferromagnetic ordering of *SmZnAsO* is observed at 4.6(2) K (Fig. 3), for *GdZnAsO* at 3.4(2) K.

In addition, ZFC-FC measurements of *REZnAsO* ($RE = \text{Ce, Pr, Nd}$) with a field strength of 100 Oe do

Table 4. Effective magnetic moment (μ_{eff} , 100–300 K) and paramagnetic Curie temperature (θ_{p}).

Compound	μ_{eff} (μ_{B} mol $^{-1}$)	θ_{p} (K)
CeZnAsO	2.46(1)	−36
PrZnAsO	3.51(1)	−20
NdZnAsO	3.34(1)	−16
GdZnAsO	8.13(1)	−14

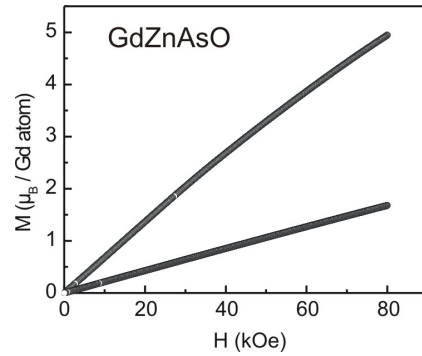


Fig. 4. Magnetization isotherms of *GdZnAsO* at 3 (top) and 50 K (bottom).

not show magnetic ordering down to the lowest reachable temperature (2 K) of our PPMS. The magnetization isotherm at 50 K of *GdZnAsO* (Fig. 4) increases almost linearly as expected for a paramagnetic material. At 3 K, slightly below the Néel temperature, the curvature becomes more pronounced, and the maximum moment observed at 3 K and 80 kOe is 4.9 μ_{B} /Gd atom.

^{121}Sb Mössbauer spectroscopy

The ^{121}Sb Mössbauer spectra of the antimonide oxides *REZnSbO* ($RE = \text{Pr, Nd}$) recorded at 77 and 4.2 K are presented in Fig. 5 together with transmission integral fits. The corresponding fitting parameters are listed in Table 5. As expected from the crystal structure the spectra could be well reproduced with single antimony sites. Owing to the high natural line width of antimony, no quadrupole moment was needed for the fits, although, for the non-cubic site symmetry ($4mm$), weak quadrupole splitting is expected.

The isomer shifts (4 K data) of -8.33 (PrZnSbO) and -8.27 mm s^{-1} (NdZnSbO), respectively -8.19 mm s^{-1} at 77 K, fit very well in the series of antimonide oxides with *ZrCuSiAs* structure investigated up to now [13]. The 4.2 K spectrum shows no line broadening caused by transferred hyperfine fields as observed for some *REMnSbO* compounds

Table 5. Fitting parameters of ^{121}Sb Mössbauer spectroscopic measurements of PrZnSbO and NdZnSbO . Numbers in parentheses represent the statistical errors in the last digit. (δ), isomer shift; (Γ), experimental line width. The 77 K data of PrZnSbO were taken from ref. [13].

Compound	T (K)	δ (mm s^{-1})	Γ (mm s^{-1})
PrZnSbO	77	$-8.37(2)$	$2.78(4)$
	4.2	$-8.33(2)$	$3.10(7)$
NdZnSbO	77	$-8.19(2)$	$2.87(5)$
	4.2	$-8.27(6)$	$3.01(2)$

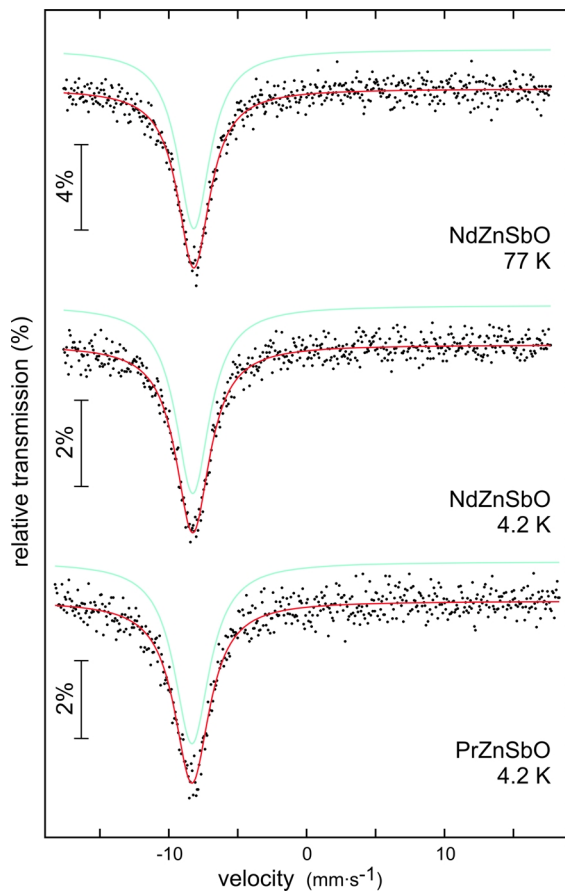


Fig. 5 (color online). Experimental and simulated ^{121}Sb Mössbauer spectra of PrZnSbO and NdZnSbO at different temperatures.

[13]. The antimonide oxides with zinc as the transition metal studied herein show similar patterns at 77 and 4.2 K.

Optical properties

The hitherto unpublished spectra of several phosphide oxides and arsenide oxides are summarized in

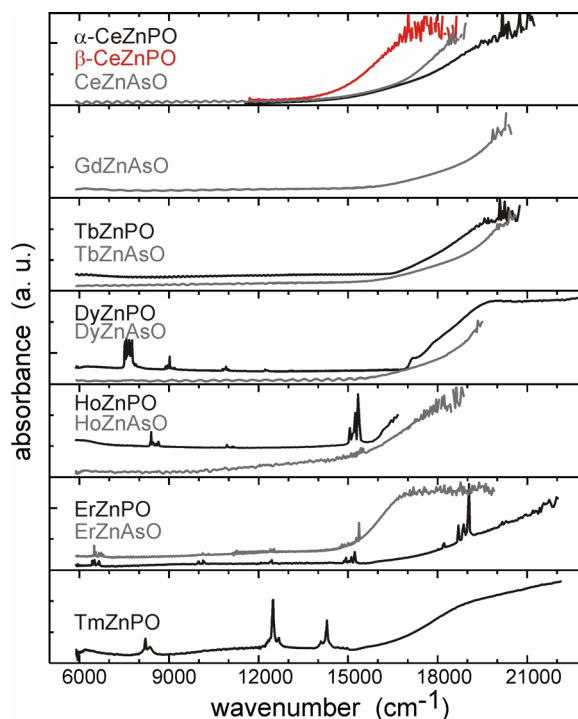


Fig. 6 (color online). Polarized single-crystal NIR/Vis electronic spectra of some phosphide oxides and arsenide oxides $REZnPnO$ ($RE = \text{Ce, Gd, Tb, Dy, Ho, Er, Tm}$; $Pn = \text{P, As}$). Polarization perpendicular to the c axis. For clarity the spectra are shifted along the ordinate axis. The spectra of DyZnPO and HoZnPO have been published earlier [11] and are given for comparison. For an assignment of the electronic transitions of ErZnPO and TmZnPO see Fig. 7 and 8, respectively.

Fig. 6. As expected, for the cerium compounds α - and β - CeZnPO and CeZnAsO no absorption due to an f - f electronic transition is observed in the spectral range under investigation. Interestingly, the lowest lying charge transfer transition, most likely $Pn^{3-} \rightarrow Zn^{2+}$, occurs for CeZnAsO just in between the energies observed for α - CeZnPO ($\tilde{\nu} \approx 18000 \text{ cm}^{-1}$) and β - CeZnPO ($\tilde{\nu} \approx 16000 \text{ cm}^{-1}$). Even for the antimonide oxides $REZnSbO$ ($RE = \text{La, Pr, Nd}$) the charge transfer transition is observed in this energy range (Fig. 9). Thus, a stronger structural than chemical influence on the energy of the charge transfer is manifested. The energy of the charge transfer transitions (optical band gap) for the other pnictide oxides in Fig. 6 are roughly in the same range, with the exception of ErZnAsO and HoZnPO .

In addition to the charge transfer transition in the spectra of TmZnPO and ErZnPO , the typical f - f elec-

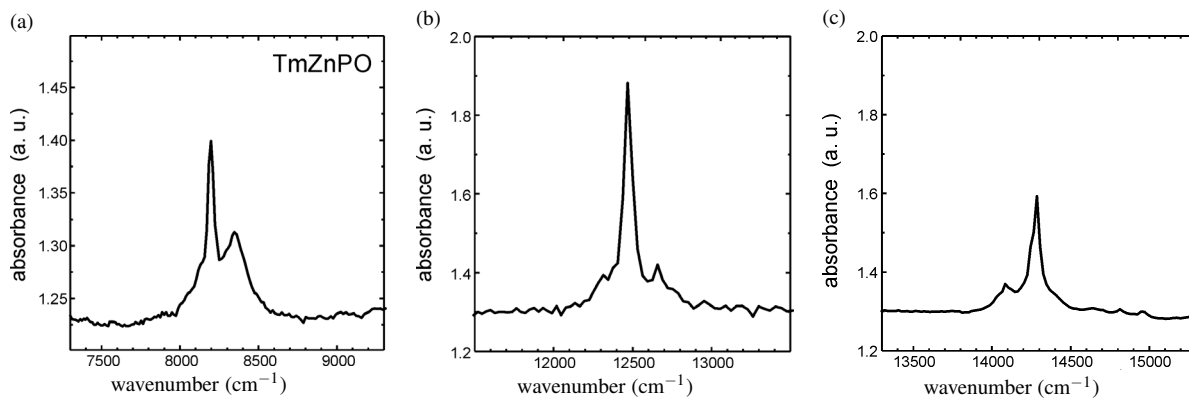


Fig. 7. Ligand-field splitting of the electronic transitions ${}^3H_6 \rightarrow {}^3H_5$ (a), 3F_4 (b), 3F_3 (c) in the NIR/Vis spectrum of TmZnPO.

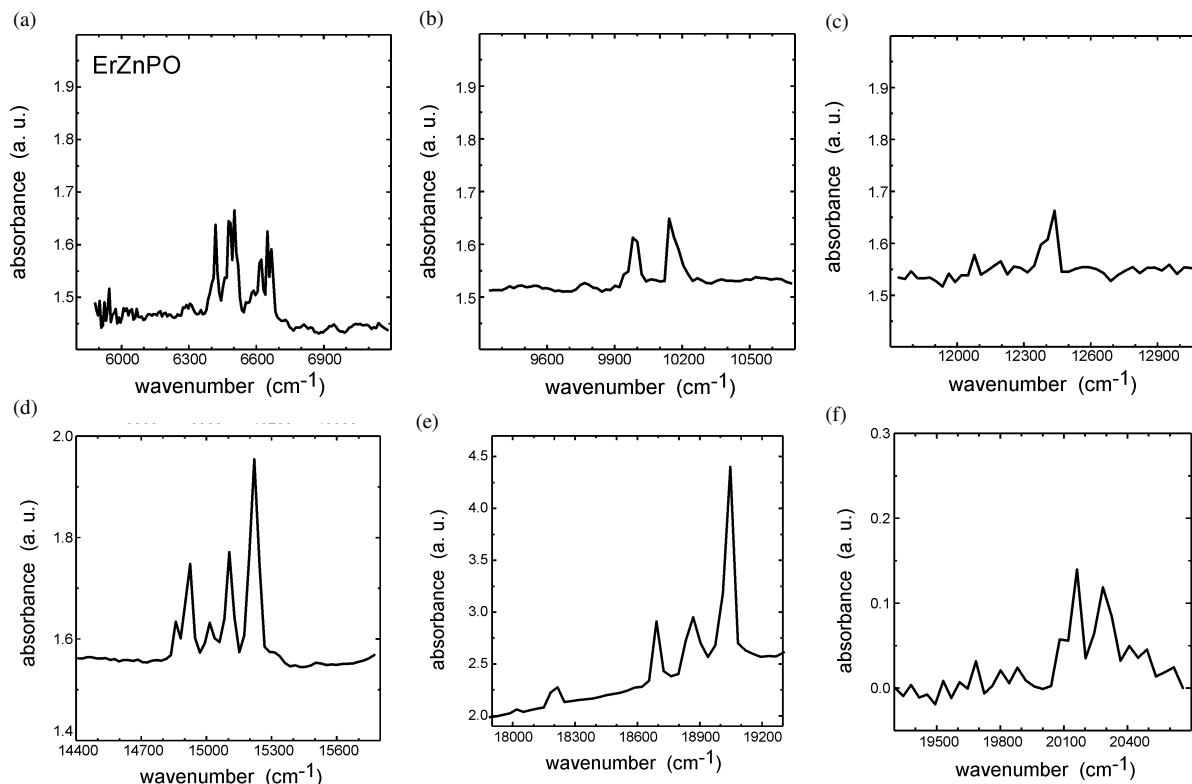


Fig. 8. Ligand-field splitting of the electronic transitions ${}^4I_{5/2} \rightarrow {}^4I_{13/2}$ (a), ${}^4I_{11/2}$ (b), ${}^4I_{9/2}$ (c), ${}^4F_{9/2}$ (d), ${}^4S_{3/2}$ and ${}^4H_{11/2}$ (e), ${}^4F_{7/2}$ (f) in the NIR/Vis spectrum of ErZnPO. For the part of the spectrum given in (f) a baseline correction has been applied, to allow better recognition of the weak signals around 20200 and 20300 cm^{-1} .

tronic transitions for Tm^{3+} (Fig. 7) and Er^{3+} (Fig. 8) can be recognized. Assignment of these electronic transitions according to the Dieke diagram [23,24] is straightforward and might be compared to that of Tm^{3+} [25] and Er^{3+} [26] in various nitrates.

Eventually, we note two peculiarities observed in the spectra of the arsenide oxides and the antimonide oxides. In general, the molar extinction of the $f-f$ electronic transitions in the arsenide oxides and even more so in the antimonide oxides is much smaller than that

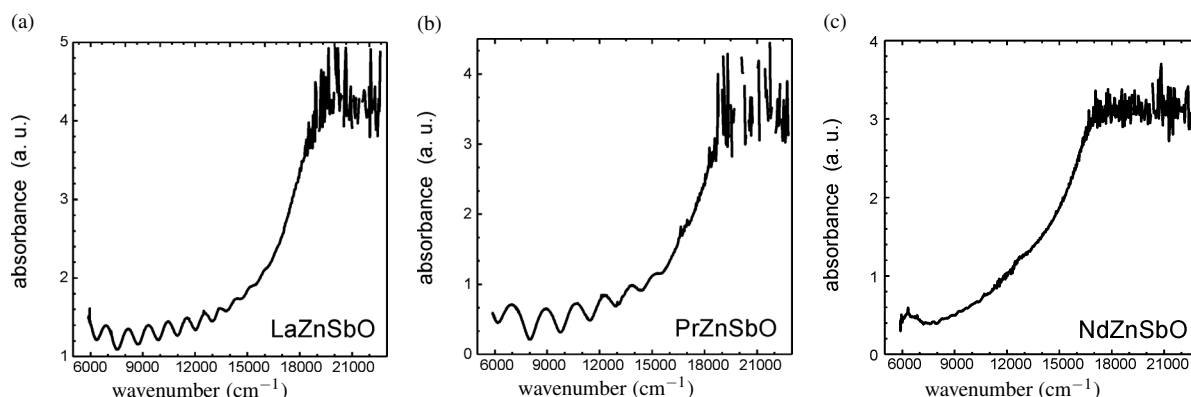


Fig. 9. Polarized single-crystal NIR/Vis electronic spectra of antimonide oxides *REZnSbO* (*RE* = La, Pr, Nd). Polarization of the incident beam perpendicular to the crystallographic *c* axis.

found for the phosphide oxides. We have no explanation for this observation. Secondly, the absorption spectra of the antimonide oxides are strongly hampered by interference effects. This is not observed for the arsenide oxides or the phosphide oxides. We attribute this distortion of the spectra to the extremely lamellar crystals of the antimonide oxides, which show very easy cleavage parallel to the *ab* plane. Thus, crystals of the antimonide oxides can act as a Fabry-Perrot

etalon [27]. Due to variations in the thickness of the lamellae no sharp interferences are generated.

Acknowledgements

This work was financially supported by the Deutsche Forschungsgemeinschaft through SPP 1458 *Hochtemperatursupraleitung in Eisenpnictiden*. W.H. and H.L. are indebted to the NRW Graduate School of Chemistry and the Fonds der Chemischen Industrie for PhD stipends.

- [1] D. Johrendt, R. Pöttgen, *Angew. Chem.* **2008**, *120*, 4860; *Angew. Chem. Int. Ed.* **2008**, *47*, 4782.
- [2] R. Pöttgen, D. Johrendt, *Z. Naturforsch.* **2008**, *63b*, 1135.
- [3] H.-H. Wen, *Adv. Mater.* **2008**, *20*, 3764.
- [4] T. C. Ozawa, S. M. Kauzlarich, *Sci. Techn. Adv. Mater.* **2008**, *9*, 033003.
- [5] M. V. Sadovskii, *Phys. Usp.* **2008**, *51*, 1243.
- [6] A. L. Ivanovski, *Phys. Usp.* **2008**, *51*, 1273.
- [7] Yu. A. Izyumov, E. Z. Kurmaev, *Phys. Usp.* **2008**, *51*, 1307.
- [8] Z.-A. Ren, W. Lu, J. Yang, W. Yi, X.-L. Shen, Z.-C. Li, G.-C. Che, X.-L. Dong, L.-L. Sun, F. Zhou, Z.-X. Zhao, *Chin. Phys. Lett.* **2008**, *25*, 2215.
- [9] H. Hiramatsu, H. Kamioka, K. Ueda, H. Ohta, T. Kamiya, M. Hirano, H. Hosono, *Phys. Stat. Sol. A* **2006**, *203*, 2800.
- [10] H. Lincke, T. Nilges, R. Pöttgen, *Z. Anorg. Allg. Chem.* **2006**, *632*, 1804.
- [11] H. Lincke, R. Glaum, V. Dittrich, M. Tegel, D. Johrendt, W. Hermes, M. H. Möller, T. Nilges, R. Pöttgen, *Z. Anorg. Allg. Chem.* **2008**, *634*, 1339.
- [12] H. Lincke, R. Glaum, V. Dittrich, M. H. Möller, R. Pöttgen, *Z. Anorg. Allg. Chem.* **2009**, *635*, 936.
- [13] I. Schellenberg, T. Nilges, R. Pöttgen, *Z. Naturforsch.* **2008**, *63b*, 834.
- [14] P. Wollesen, J. W. Kaiser, W. Jeitschko, *Z. Naturforsch.* **1997**, *52b*, 1467.
- [15] A. T. Nientiedt, W. Jeitschko, *Inorg. Chem.* **1998**, *37*, 386.
- [16] Y. Takano, S. Komatsuzaki, H. Komasaki, T. Watanabe, Y. Takahashi, K. Takase, *J. Alloys Compd.* **2008**, *451*, 467.
- [17] R. Pöttgen, Th. Gulden, A. Simon, *GIT Labor-Fachzeitschrift* **1999**, *43*, 133.
- [18] K. Yvon, W. Jeitschko, E. Parthé, *J. Appl. Crystallogr.* **1977**, *10*, 73.
- [19] G. M. Sheldrick, SHELXL-97, Program for Crystal Structure Refinement, University of Göttingen, Göttingen (Germany) **1997**; see also: G. M. Sheldrick, *Acta Crystallogr.* **2008**, *A64*, 112.
- [20] E. Krausz, *AOS News* **1998**, *12*, 21.
- [21] E. Krausz, *Aust. J. Chem.* **1993**, *46*, 1041.
- [22] R. A. Brand, NORMOS, Mössbauer fitting Program, Universität Duisburg, Duisburg (Germany) **2007**.
- [23] G. H. Dieke, *Spectra and Energy Levels of the Rare Earth Ions in Crystals*, Wiley Interscience, New York **1968**.

- [24] B. Henderson, G. F. Imbusch, *Optical Spectroscopy of Inorganic Solids*, Clarendon, Oxford **1989**.
- [25] S. V. J. Lakshman, C. K. Jayasankar, *J. Phys. C: Solid State Phys.* **1984**, *17*, 2967.
- [26] S. V. J. Lakshman, C. K. Jayasankar, *Pramāna* **1984**, *23*, 129.
- [27] D. Meschede, *Optik, Licht und Laser*, B. G. Teubner Verlag, Wiesbaden **2005**.